中國機械工程學刊第四十一卷第五期第 595~604 頁(民國一百零九年)
Journal of the Chinese Society of Mechanical Engineers, Vol.41, No.5, pp 595~604 (2020)

Mechanical-Electric-Hydraulic Coupling Dynamics of Hydraulic Drilling Rig

Guangzhu Chen*, Chenglin Jiang**, Changwei Miao**, Lin Fu*** and Liangzhao Qi**

Keywords： hydraulic drilling rig, mechanical-electrical-hydraulic coupling, dynamics analysis, hydraulic motor leakage, sensitivity analysis

ABSTRACT

The coupling relationship of the hydraulic drilling rig, as a complex mechanical system with mechanical-electric-hydraulic, is very important to its working performance. The internal leakage of the hydraulic motor (a direct drive component of the drilling rig) is easy to appear and difficult to be directly observed, so it is especially important to analyze the working performance of the drilling rig under the internal leakage condition of the hydraulic motor. This paper focuses on the analysis of mechanical-electric-hydraulic dynamics of hydraulic drilling rig under no loading and loading. Firstly, a coupling dynamics model of the drilling rig is established theoretically and then the dynamic response of the drilling rig is analyzed by simulation. Secondly, the leakage sensitivity simulation and analysis of hydraulic motor is performed to explore the impact of the internal leakage of the hydraulic motor on the dynamic response of the drilling rig. Finally, a dynamic response test platform of the drilling rig is built, the experiment result agrees better with the simulation result under different leakage ratios of the hydraulic motor, and the leakage ratio of the hydraulic motor is sensitive to the rotational speed and load torque of the drilling rig.

Paper Received November, 2017. Revised February, 2019, Accepted September, 2018, Author for Correspondence: Guangzhu Chen.

* *Professor, College of Nuclear Technology and Automation Engineering, Chengdu University of Technology, Chengdu 610065, P.R.China.*

** *Graduate Student, College of Nuclear Technology and Automation Engineering, Chengdu University of Technology, Chengdu 610065, P.R.China.*

*** *Lecturer, College of Nuclear Technology and Automation Engineering, Chengdu University of Technology, Chengdu 610065, P.R.China.*

INTRODUCTION

With development of industry technology, the mechanical-electric-hydraulic machine has been already widely used in manufacturing, military, mining, agriculture and other fields.it is very important to analogy the mechanical-electric-hydraulic coupling relation of the machine, which helps to master its operation rules and put forward the corresponding control strategy. At pre-sent, the research methods on electro-mechanical-hydraulic coupling dynamics are mainly divided into two aspects: one is to establish the mathematical model of system coupling dynamics based on the dynamic model of mechanical, electrical and hydraulic components, so as to analyze system dynamic characteristics; the other is to analyze its dynamic characteristics directly by using simulation software, such as ADAMS and AMESim.

A nonlinear dynamic coupled model for hydropower station system, which contained the model of water-carriage system, water turbine system, speed governor system, generator’s electromagnetic system, grid, shaft system of hydroelectric generating set, as well as the powerhouse, was established in Wu, et al. (2017). Qi, et al. (2017) established respectively the virtual prototype model and the hydraulic circuit model of the lifting platform of an anti-riot vehicle based on ADAMS and AMESim, and the analysis was carried out by an co-simulation. Yang, et al. (2018) con-ducted a fundamental study on hydraulic-mechanical-electrical coupling mechanism for small signal stability of hydropower plants (HPPs), and analyzed the impact of hydraulic-mechanical factors on the local mode oscillation in a Single-Machine-Infinite-Bus system. Meng, et al. (2018) presented a mathematical model for pose monitoring and control of the hydraulic support, and established a mechanical-electrical-hydraulic co-simulation numerical model, a teaching-learning-based optimization algorithm (TLBO) was then introduced to obtain the numerical solution of the nonlinear equations, the results indicated the mechanical-electrical-hydraulic co-simulation approach was effective for describing the hydraulic support.

Through above analysis, it can be seen that the effect of mechanical-electrical-hydraulic coupling relation on the equipment dynamic response can't be ignored and must be considered. The hydraulic drilling rig, hereinafter referred to as drilling rig, with compact structure, stable transmission and easy speed change advantages has been widely used to drilling operation in many fields such as construction engineering, geology exploration and mining industry. As a complex mechanical-electric-hydraulic system, the coupling relationship of mechanical, electrical and hydraulic components of the drilling rig affects the output load torque and rotational speed of the drilling process.

Wang, et al. (2014) studied the influence of the dynamic characteristics of hydraulic system on the performance of the full hydraulic directional drilling rig by simulation, a coupled dynamic model of the drilling rig gear transmission system was built using the lumped-parameter meth-od, and then the vibration responses of the system were also studied (Wang, et al., 2014). Xin, et al. (2013) studied and optimized the dynamic performance of the clamping hydraulic circuit of the drilling rig by using the load self-adaptation principle. In order to improve the load adaptability of the directional drilling rig, Zhang, et al. (2012) designed a hydraulic system with load sensing, and further analyzed its dynamic characteristics. Flexible multibody dynamics (FMBD) based on the absolute nodal coordinate formulation (ANCF) is adapted for the mathematical modeling of the risers and joints of a semisubmersible drilling rig(Ham, et al., 2017), the motion analysis with and without connections was fulfilled to verify the effect of connectivity.

The internal leakage of a hydraulic motor (a direct drive component of a drilling rig) is one of the key factors which directly influence the output load torque and rotational speed performance of the drilling rig. But it is difficult to observe directly the leakage phenomenon and master the working rules of a hydraulic motor due to the concealment of the leakage phenomenon. Wang, et al. (2016) established a flow field inside a hydraulic motor, which ignored the gap between the blade and the blade groove, and a hydraulic motor fluid model in different working conditions, then using ANSYS ICEM CFD tool to generate high-quality O-Net mesh for meeting the computing requirements, and the flow field inside the hydraulic motor was simulated using fluid simulation software-CFX. Wen, et al. (2017) put forward a new type of double-stator swing hydraulic motor, and the geometric displacement calculation formulas of inner and outer hydraulic motors were summed up and the main internal leakage paths were analyzed through the analysis of the internal structure of double-stator swing hydraulic motor, then, every leakage of inner and outer hydraulic motors was calculated theoretically, at the same time, a seal structure optimization program was also put forward.

Wang, et al. (2018) established a mathematical models of the internal leakage of continuous rotary electro-hydraulic servo hydraulic motor, and then simulation analysis was implemented on the continuous rotary electro-hydraulic servo hydraulic motor by the finite element analysis software ANSYS based on the fluid-structure interaction theory, the results showed the deformation of hydraulic motor's key parts and the changing rule of internal leakage.

In this paper, mechanical-electrical-hydraulic coupling dynamic characteristics of drilling rig will be studied to found the coupling relationships among sub-systems (electric control system, mechanical system and hydraulic system).Firstly a mechanical-electrical-hydraulic coupling dynamics model of drilling rig is established based on the torque balance equation of reducer, mathematical model of Load-sensing proportional directional valve and mathematical model of speed control system of hydraulic motor. Then a dynamics characteristics simulation analysis under unload stage and load stage, especially sensitivity analysis un-der different leakage ratios of the hydraulic motor was conducted. Finally, Experimental verification of mechanical-electrical-hydraulic coupling dynamics model and sensitivity of the hydraulic motor leakage ratio to the rotational speed and load torque of the drilling rig are built.

MECHANICAL-ELECTRICAL-HYDRAULIC COUPLING DYNAM-ICS MODEL OF DRILLING RIG

Structure and Working Principle of Drilling Rig

The drilling rig shown in Fig.1 mainly consists of three parts: host machine, hydraulic system and control system. The host machine is composed of hydraulic motor, reducer, hydraulic chuck, hydraulic gripper, feed cylinder and machine frame. The hydraulic system is mainly com-posed of tank, load-sensing proportional directional vale, hydraulic pump and solenoid valves. While the control system is mainly composed of programmable logic controller (PLC) and various operation buttons to control the action of host machine, hydraulic system. In a word, the hydraulic system is controlled by receiving instruction from the control system to drive the host machine to perform series of drilling actions. All actions of the host machine are realized by four hydraulic circuits, which include the rotation circuit, feed circuit, chuck circuit and gripper circuit. Four hydraulic circuits of the drilling rig are shown in Fig.2. In order to master the output response of the drilling rig completely, the dynamic characteristics of all hydraulic circuits should be analyzed. Be-cause the analysis process and modeling approach are similar for four hydraulic circuits, and the rotation circuit is the main and most complicated working circuit in the drilling rig, the rotation circuit has been chosen as the research object for mechanical-electrical-hydraulic coupling dynamics analysis of the drilling rig in this paper.

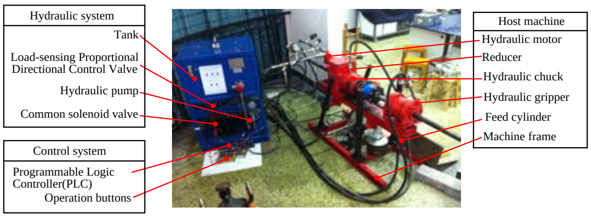

Figure 1. Structure of drilling rig.

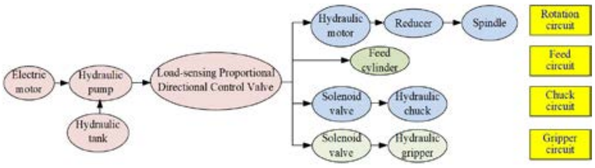

Figure 2. Four hydraulic circuits of drilling rig.

There are two kinds of working states (unload state and load state) for the drilling rig in actual working period. In unload state, the drilling tool of the drilling rig has not contacted the rock, so the output load torque value of the drilling rig is close to zero at this time. When the drilling rig is in the load state, the drilling rig has begun to drill the rock, and the output load torque value of the drilling rig is equal to the actual load required torque value of broking the rock.

Torque Balance Equation of Reducer

The dynamics model of the reducer can be simplified as a mass-damping system shown in Fig.3. The moment balance equation of the reducer's input shaft can be ex-pressed as

$$T_i(t) = J_i \frac{\mathrm{d}\omega_i(t)}{\mathrm{d}t} + B_i\omega_i(t) + T(t) \tag{1}$$

where $T_i(t)$ is the output torque of the hydraulic motor (N·m), namely the output load torque of the drilling rig, J_i is the moment of inertia of the input shaft (kg·m^2), $\omega_i(t)$ is the rotational speed of the hydraulic motor (rad/s), B_i is the viscous damping coefficient of the input shaft (N·m·s/rad), $T(t)$ is the equivalent torque of the gear pair (N·m).

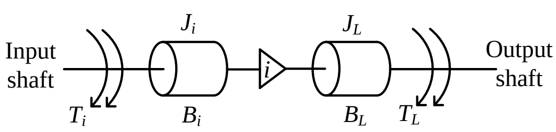

Figure 3. Dynamics model of reducer.

Similarly, the moment balance equation of the reducer's output shaft can be express as

$$iT(t) = J_L \frac{\mathrm{d}\omega_L(t)}{\mathrm{d}t} + B_L\omega_L(t) + T_L(t) \tag{2}$$

where i is the transmission ratio of the reducer, J_L is the moment of inertia of the output shaft (kg·m^2), $\omega_L(t)$ is the rotational speed of the output shaft (rad/s), B_L is the viscous damping ratio of the output shaft (N·m·s/rad), $T_L(t)$ is the torque of the output shaft (N·m).

Due to $\omega_L(t) = \omega_i(t)/i$, $\omega_i(t)$ and $T_L(t)$ can be eliminated by simultaneously solving Eqs. (1) and (2), and the following equation can be acquired

$$T_i(t) = (iJ_i + \frac{J_L}{i})\frac{\mathrm{d}\omega_L(t)}{\mathrm{d}t} + (iB_i + \frac{B_L}{i})\omega_L(t) + \frac{T_L(t)}{i} \tag{3}$$

Here, $J_e = iJ_i + J_L / i$ is defined as the equivalent moment of inertia of the reducer and $B_e = iB_i + B_L / i$ is defined as the equivalent damping ratio of the reducer, then Eq. (3) can be further simplified as

$$T_i(t) = J_e \frac{\mathrm{d}\omega_L(t)}{\mathrm{d}t} + B_e\omega_L(t) + \frac{T_L(t)}{i} \tag{4}$$

By Laplace transform, Eq. (4) can be transformed into

$$T_i(s) = J_e s\omega_L(s) + B_e\omega_L(s) + \frac{T_L(s)}{i} \tag{5}$$

Modeling of Load-sensing Proportional Directional Valve

Load-sensing proportional directional valve is used in the hydraulic system in order to reduce energy consumption. Due to the load sensitivity of the valve was not considered, here only the electro-hydraulic proportional control characteristics of the load-sensing proportional directional valve for the rotation hydraulic circuit was analyzed based on mathematical modeling.

When the proportional solenoid of the load-sensing proportional directional valve works in the linear range, whose output characteristics can be approximated as Eqs. (6) and (7).

$$F_d(t) = K_I I(t) - K_y X_V(t) \tag{6}$$

$$m\frac{\mathrm{d}^2 X_V(t)}{\mathrm{d}t^2} + D\frac{\mathrm{d}X_V(t)}{\mathrm{d}t} + K_{sy}X_V(t) = F_d(t) \tag{7}$$

where $F_d(t)$ is the output force of the proportional solenoid (N), K_I is the current-force gain ratio of the proportional solenoid (N/mA), $I(t)$ is the control current of the load-sensing proportional directional valve (mA), $X_V(t)$ is the displacement of the valve core (m), and $K_y = \partial F_d(t)/\partial X + K_{sy}$ is the total stiffness of the proportional solenoid (N/m), which is the sum of displacement-force gain of the proportional solenoid $\partial F_d(t)/\partial X$ and the zero spring stiffness of the proportional solenoid K_{sy} (N/m), m is the quality of the valve core (kg), D is the motion damping ratio of the valve core (N/m/s).

By Laplace transform, Eqs. (6) and (7) are transformed into Eqs. (8) and (9), respectively.

$$F_d(s) = K_I I(s) - K_y X_V(s) \tag{8}$$

$$ms^2 X_V(s) + DsX_V(s) + K_{sy} X_V(s) = F_d(s) \tag{9}$$

By solving Eqs. (8) and (9) simultaneously, the model equation of the proportional solenoid of the load-sensing proportional directional valve can be expressed as

$$I(s) = \frac{ms^2 + Ds + K_{sy} + K_y}{K_I} X_V(s) \tag{10}$$

The linearized flow continuity equation of the load-sensing proportional directional valve is

$$Q_L(t) = K_q X_V(t) - K_c P_L(t) \tag{11}$$

where $Q_L(t)$ is the flow of the valve body (m^3/s), K_q is the flow gain ratio of the valve body (m^2/s), K_c is the flow-pressure ratio of the valve body (m^3/s·Pa), $P_L(t)$ is the outlet load pressure of the valve body.

By Laplace transform on Eq. (11), the flow continuity equation of the load-sensing proportional directional valve can be expressed as

$$Q_L(s) = K_q X_V(s) - K_c P_L(s) \tag{12}$$

Modeling of Rotational Speed Governing System of Hydraulic motor

Considering the internal leakage and the external leakage of the hydraulic motor, the flow continuity equation of two hydraulic motor's chambers can be expressed as

$$Q_L(t) = D_m \omega_m(t) + C_{tm} P_L(t) + \frac{V_m}{\beta_e} \times \frac{\mathrm{d}P_L(t)}{\mathrm{d}t} \tag{13}$$

where D_m is the theoretical swept volume of the hydraulic motor (m^3/rad), $\omega_m(t)$ is the rotational speed of the hydraulic motor (rad/s), C_{tm} is the leakage coefficient of the hydraulic motor (m^3/s/Pa), $P_L(t)$ is the working pressure of the hydraulic motor (Pa), V_m is the volume of the high-pressure chamber (m^3), β_e is the bulk modulus of hydraulic oil (Pa).

The torque balance equation of the hydraulic motor's the output shaft can be expressed as

$$T_m(t) = J_m \frac{\mathrm{d}\omega_m(t)}{\mathrm{d}t} + B_m \omega_m(t) + T_i(t) \tag{14}$$

where J_m is the moment of inertia of the hydraulic motor's the output shaft (kg·m^2), B_m is the viscous damping coefficient of the hydraulic motor (N·m·s/rad), $T_i(t)$ is the load torque acting on the hydraulic motor's the output shaft (N·m).

By Laplace transform, Eqs. (13) and (14) can be transformed into Eqs. (15) and (16), respectively.

$$Q_L(s) = D_m \omega_m(s) + C_{tm} P_L(s) + \frac{V_m}{\beta_e} sP_L(s) \tag{15}$$

$$P_L(s) D_m = J_m s \omega_m(s) + B_m \omega_m(s) + T_i(s) \tag{16}$$

Modeling of Mechanical-Electrical-Hydraulic Coupling Dynamics

Five basic equations (Eqs. (5), (10), (12), (15) and (16)) of the drilling rig are related to the change of the physical quantity under initial conditions, and also used to analyze the dynamic characteristics of the rotation hydraulic circuit.

Now, assuming that the mechanical transmission system of the drilling rig is completely rigid, so the following equation can be established, as Eq. (17).

$$\begin{cases} \omega_m(s) = \omega_i(s) \\ \omega_L(s) = \omega_i(s)/i \end{cases} \tag{17}$$

Based on Eq. (17), the relationship between $\omega_m(s)$ and $\omega_L(s)$ can be described as

$$\omega_m(s) = i\omega_L(s) \tag{18}$$

By simultaneously solving Eqs. (5), (10), (12), Eqs. (15), (16) and (18), the mechanical-electrical-hydraulic coupling dynamic model of the drilling rig can be described as

$$\omega_L(s) = \frac{\dfrac{K_\mathrm{I}}{ms^2 + Ds + K_{sy} + K_y} I(s) - \dfrac{V_m s + \beta_e (C_{tm} + K_c)}{i\beta_e D_m K_\mathrm{q}} T_L(s)}{\dfrac{J_d V_m}{\beta_e K_q D_m} s^2 + \dfrac{J_d \beta_e (C_{tm} + K_c) + B_d V_m}{\beta_e K_q D_m} s + \dfrac{iD_m^2 + B_d (C_{tm} + K_c)}{K_q D_m}} \tag{19}$$

where B_d is the equivalent viscous damping ratio of the power unit (N·m·s/rad), and $B_d = iB_m + B_e$.

It can be known that the rotation hydraulic circuit of the drilling rig can be regarded as a system with two inputs and one output through Eq. (19),namely, the rotational speed of the drilling rig $\omega_L(s)$ is mainly affected by the control current of the load-sensing proportional directional valve $I(s)$ and the load torque of the drilling rig $T_L(s)$.

DYNAMICS CHARACTERISTICS SIMULATION AND ANALYSIS OF DRILLING RIG

Dynamic Response Simulation and Analysis of Drilling Rig

In order to solve the coupling dynamics model described by Eq. (19), all the constant parameter values in Eq. (19) must be determined firstly. Generally, the parameter values of the mechanical-electrical-hydraulic coupling dynamics model of the drilling rig are obtained through experimental analysis, and shown in Table 1.

Table 1. Parameter values of mechanical-electrical-hydraulic coupling dynamics model of the drilling rig.

Parameter	i	J_i (kg·m^2)	J_L (kg·m^2)	J_e (kg·m^2)
Value	1.194	0.041	2.02	1.74
Parameter	B_i (N·m·s/rad)	B_L (N·m·s/rad)	K_I (N/mA)	K_{sy} (N/mm)
Value	0.5	0.5	0.55	10
Parameter	B_e (N·m·s/rad)	K_y (N/mA)	m (kg)	D (N/m/s)
Value	0.61	24	0.15	0.3
Parameter	K_q (m^2/s)	K_c (m^3/s·Pa)	β_e (Pa)	D_m (m^3/rad)
Value	0.0081	1.2×10^{-11}	7.5×10^{8}	2.5×10^{-5}
Parameter	C_{im} (m^3/s/Pa)	C_{em} (m^3/s/Pa)	C_{tm} (m^3/s/Pa)	V_m (m^3)
Value	0.58×10^{-14}	0.35×10^{-14}	1.28×10^{-14}	1.2×10^{-3}
Parameter	J_m (kg·m^2)	B_m (N·m·s/rad)	J_d (kg·m^2)	B_d (N·m·s/rad)
Value	6.7×10^{-4}	0.5	1.74	1.61

As mentioned in section 2.5, the mechanical-electrical-hydraulic coupling dynamics model of the drilling rig is a system with two inputs and one output. As the input of the system, the control current of the proportional directional valve and the load torque of the drilling rig are treated as step signals, shown in Fig.4.

It can be observed that the magnitude and corresponding jump time of the control current are 630mA and 1s, respectively, while the two values of the load torque are 50N and 4s, respectively. The input signal rule shows that the drilling rig will not work until the control current is switched on at 1s. Then, it will run in unload state during 1~4s time because its load torque is zero during this time. Finally, the load torque appears and the drilling rig will work in load state after 4s time. The load torque value 50N·m is the load torque value in simulation period.

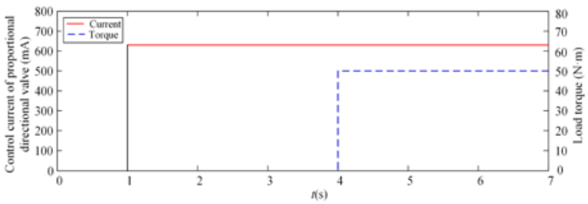

Figure 4. Input signal curves of the coupling dynamics model.

MATLAB/Simulink software is adapted to finish the simulation process. The rotational speed of the drilling rig is shown in Fig.5.

It can be observed that the rotational speed of the drilling rig is 0 in 0~1s time, that's because the drilling rig doesn't yet work. In 1s~4s time, the drilling rig begins to work under unload condition, so its rotational speed increases sharply at 1s time and then fluctuates until stabilizing around 26r/min under the viscous damping. The output rotation speed of the drilling rig decreases sharply at 4s time due to the snap load effect, and then fluctuates until stabilizing around 19r/min under the function of the viscous damping and load torque. Fig.5 also shows that the rotational speed of the drilling rig will decrease significantly after loading 50N·m.

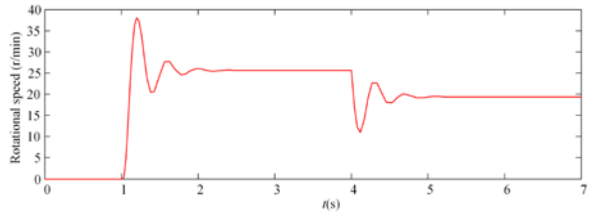

Figure 5. Response curve of mechanical-electrical-hydraulic coupling dynamics model of drilling rig.

Leakage Sensitivity Simulation and Analysis of Hydraulic Motor

There exits usually oil leakage in the hydraulic motor, which is mainly caused by the component wear and pipe joint looseness. The leakage coefficient of the hydraulic motor is generally used to judge the leakage level of the hydraulic motor. Because the oil leakage of the hydraulic motor means the existence of energy loss in the hydraulic system, it will have an influence on the output performance of the drilling rig.

When the leakage flow of the hydraulic motor is less than 0.0002% ($C_{tm}\leq1.2\times10^{-14}$) of the maximum working flow, leakage phenomenon is negligible. So $C_{tm}=1.2\times10^{-14}$ is a critical value which judges whether there is leakage phenomenon of the hydraulic motor. In order to analyze the leakage sensitivity of the hydraulic motor to the working performance of the drilling rig, the hydraulic motor leakage flow were set as 0.0002%, 5% ($C_{tm}=3.3\times10^{-12}$) and 10% ($C_{tm}=6.5\times10^{-12}$) of the maximum working flow, respectively. 0.0002%, 5% and 10% are called leakage ratios. The rotational speeds of the drilling rig under different leakage ratios of the hydraulic motor are shown in Fig.6.

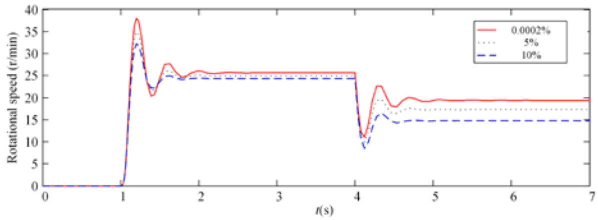

Figure 6. Rotational speeds of drilling rig under different leakage ratios of hydraulic motor.

From Fig.6, we see that:

(a) When the drilling rig works in unload state (1~4s time), the pressure of the hydraulic system is low and the leakage phenomenon is not very significant, so the leakage ratio of the hydraulic motor has a smaller influence on the rotational speeds of drilling rig. But in load state (4-7s time), the leakage will increase significantly because of increasing system pressure, so the effect of the leakage ratio of the hydraulic motor on the stable output also increases.

(b)With the increase of the leakage ratio of the hydraulic motor, the rotational speeds of the drilling rig will decrease correspondingly.

Limited to space, Fig.4, Fig.5 and Fig.6 only list the change process in 0-7s time, and the change process after 7s time are almost the same as 7th s time, respectively.

DYNAMICS CHARACTERISTICS EXPERIMENT OF DRILLING RIG

Test platform of Drilling Rig

The test platform here is almost identical in structure to the actual machine, shown in Fig.7. Some sensors such as flowmeter, pressure transmitter and torque sensor are installed on the drilling rig to measure its physical and mechanics parameters. Specifically, a wireless torque sensor is installed on the drilling pipe of the host machine to capture the load torque signal in real time. Major parameters of key components of test platform are listed in Table 2.

Table 2. Major parameters of key components of test platform

Plunger pump			load-sensing proportional directional valve		
Product model	Rated pressure	Rated swept volume	Product model	Rated pressure	Rated flow
PVB6-RSY-20	21MPa	12mL/r	HLPSL 3C1C	10MPa	6L/min
Cycloid hydraulic motor			Pressure transmitter		
Product model	Rated pressure	Rated swept volume	Product model	Measuring range	Output
2K-160	15MPa	157.2mL/r	MIK-PX300	0-20MPa	4-20mA
Explosion proof hydraulic motor			Controller		
Product model	Power	Rated speed	Product model	I/O	Output mode
YB2-100L2-4	3kw	1500r/min	S7-200-CPU226	24DI/16DO	Relay output
Flowmeter			Torque sensor		
Product model	Measuring range	Output	Product model	Measuring range	Output
LWGY-MIK-DN10	0.2-1.2m³/h	4-20mA	WYB-1000	0-1000N.m 0-3000r/min	0-3.3V

The hydraulic circuit in internal leakage test schematic diagram contains two parallel lines, of which one is com-posed of a hydraulic motor and a flowmeter, and another is composed of a globe valve and a throttle. When both the globe valve and throttle are closed, all hydraulic oil from the oil inlet will flow into the hydraulic motor and then flow back into the oil tank through the load-sensing proportional directional valve. When both the globe valve and throttle are opened, only part of the hydraulic oil from the oil inlet will flow into the hydraulic motor, while the leaked oil will flow back into the oil tank through the globe valve and throttle. Therefore, the leak-age phenomenon of the hydraulic motor may be simulated in this way, and the leakage amount can be adjusted by changing the opening size of the throttle. The flow-meter (2) placed in the oil outlet of the hydraulic motor is used to measure the flow rate of the hydraulic motor, and another flowmeter (3) placed in the common oil inlet of two parallel lines is used to measure the total flow rate of the simulated hydraulic circuit. The leakage amount of the hydraulic motor can be acquired indirectly by flow data measured by two flowmeters.

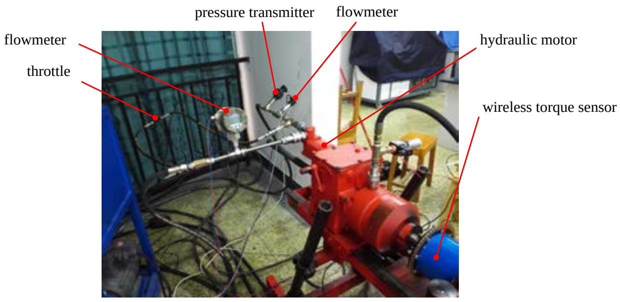

(a) Test scene

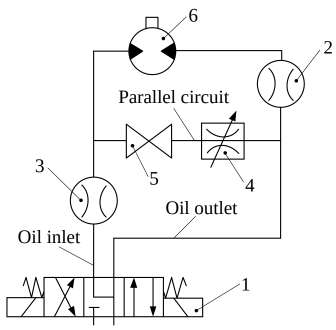

(b) Internal leakage test schematic diagram of hydraulic motor

1- load-sensing proportional directional valve; 2, 3- flowmeter; 4- throttle; 5- globe valve; 6-hydraulic motor

Figure 7. Test platform of Drilling Rig.

Experimental Results Analysis

(1) Experimental verification of mechanical-electrical-hydraulic coupling dynamics model of the drilling rig.

When there exists no leakage of the hydraulic motor, the rotational speed and load torque of the drilling rig are measured by the wireless torque sensor, and experimental results are shown in Fig.8 and Fig.9, respectively. By the statistics, it's known that the mean rotational speed and load torque of the drilling rig are 23.3r/min and 0N·m, respectively in unload stage (0~40s time), while the two values become to be 18.1r/min and 55·6N·m, respectively in load stage (40~65s time). The rotational speed of the drilling rig decreases sharply at 40s time under suddenly loaded, which is in accordance with the phenomenon described in Fig.5.

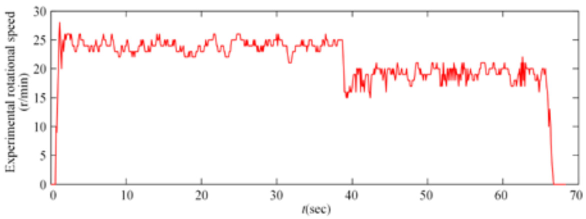

Figure 8. Rotational speed of drilling rig with no hydraulic motor leakage

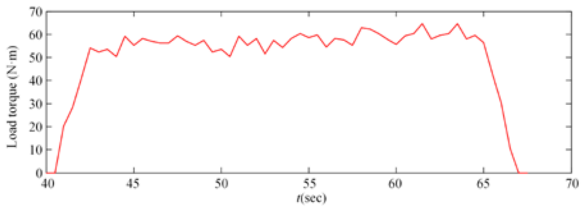

Figure 9. Load torque of drilling rig with no hydraulic motor leakage

For comparison, the simulation data (shown in Fig.5 and Fig.6) and the experiment data (shown in Fig.8 and Fig.9) are analyzed statistically, and the results are listed in Table 3.

From Table 3, it can be seen that:

(a)In unload stage with no hydraulic motor leakage, the simulation and experiment values of the rotational speed are 26.6r/min and 23.3r/min, respectively.

(b)In load stage with no hydraulic motor leakage, the simulation and experiment values of the load torque are 50N·m and 55.6N·m, respectively, while of the rotational speed 19.9r/min and 9.05%, respectively.

The above analysis showed that the experiment and the simulation results are coincident approximately (difference value is about 10%), so it can be assumed that the mechanical-electrical-hydraulic coupling dynamic model is correct and the simulation result is reliable.

Table 3. Simulation and experiment results with no hydraulic motor leakage

Load condition	Load torque (N·m)		
	Simulation value	Experiment value	Difference value
Unload stage	0	0	0%
Load stage	50	55.6	11.2%
Load condition	Rotational speed (r/min)		
	Simulation value	Experiment value	Difference value
Unload stage	26.6	23.3	12.41%
Load stage	19.9	18.1	9.05%

(2) Leakage sensitivity experimental analysis of hydraulic motor in load stage

1) Inlet flow change of the hydraulic motor

When there exists no leakage of the hydraulic motor, the inlet flow curve of the hydraulic motor in load stage is shown in Fig.10. By statistics, the average inlet flow value of the hydraulic motor is 4.56L/min.

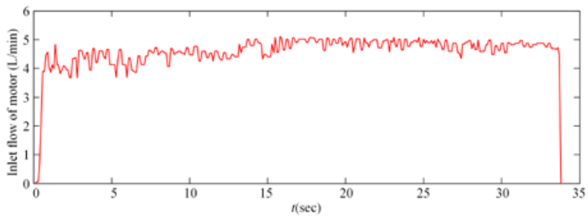

Figure 10. Inlet flow curve of the hydraulic motor with no hydraulic motor leakage in load stage

When there exists leakage of the hydraulic motor, the outlet flow curves of the hydraulic motor in load stage are shown in Fig.11. By statistics, the average outlet flow value of the hydraulic motor with 5% theoretical leakage ratio is 4.30L/min, and the measured leakage ratio of the hydraulic motor is 5.7%. Meanwhile, the average outlet flow of the hydraulic motor with 10% theoretical leakage ratio is 4.03 L/min, and the measured leakage ratio of the hydraulic motor is 11.6%.

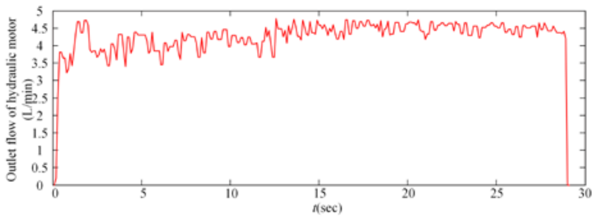

(a) 5% theoretical leakage ratio of hydraulic motor

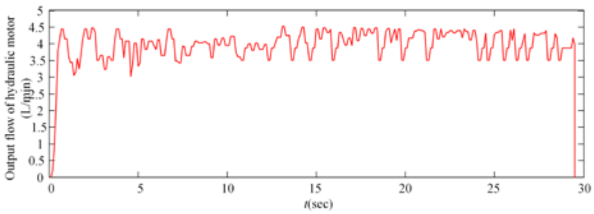

(b) 10% theoretical leakage ratio of hydraulic motor

Figure 11. Outlet flow curves of hydraulic motor with different leakage ratio in load stage

2)Rotational speed and load torque changes of the drilling rig

In load stage, the rotational speed curves and load torque curves of the drilling rig under different hydraulic motor leakage ratios are shown in Fig.12 and Fig.13, respectively. By statistics, the average rotational speed and load torque of the drilling rig are 15.6r/min and 54.7N.m, respectively under 5% theoretical leakage ratio, while 14.2r/min and 53.5N.m, respectively under 10% theoretical leakage ratio.

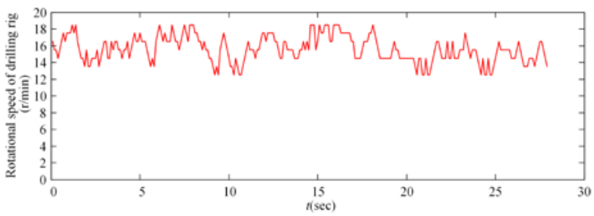

(a) 5% theoretical leakage ratio of hydraulic motor

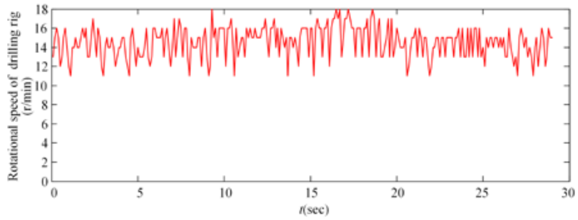

(b) 10% theoretical leakage ratio of hydraulic motor

Figure 12. Rotational speed of drilling rig under different hydraulic motor leakage ratios in load stage

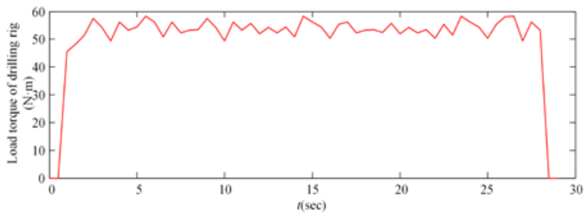

(a) 5% theoretical leakage ratio of hydraulic motor

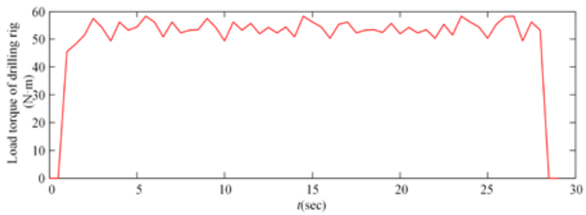

(b) 10% theoretical leakage ratio of hydraulic motor

Figure 13. Load torque of drilling rig under different hydraulic motor leakage ratios in load stage

For comparison, the simulation data (shown in Fig.5 and Fig.6) and the experiment data (shown in Fig.12 and Fig.13) were analyzed statistically, and the statistical result is listed in Table 4.

From Table 4, it can be seen that:

(a) In load stage, when hydraulic motor theoretical leakage ratios are 5% and 10%, while measured leakage ratios 5.7% and 11.6%, respectively.

(b) In load stage, the simulation and experiment values of the rotational speed are 17.3r/min and 15.6r/min, respectively under 5% theoretical leakage ratio of hydraulic motor, while 14.7 r/min and 14.2 r/min, respectively under 10% theoretical leakage ratio of hydraulic motor.

(c) In load stage, the simulation and experiment values of the load torque are 50N·m and 54.7N·m, respectively under 5% theoretical leakage ratio of hydraulic motor, while 50N·m and 53.5N·m respectively under 10% theoretical leakage ratio of hydraulic motor.

Table 4. Simulation and experiment results under different hydraulic motor leakage condition

Leakage condition	Leakage ratio		
	Simulation value	Experiment value	Difference
5% Leakage	5%	5.7%	14%
10% Leakage	10%	11.6%	16%
Leakage condition	Rotational speed (r/min)		
	Simulation value	Experiment value	Difference
5% Leakage	17.3	15.6	9.8%
10% Leakage	14.7	14.2	3.4%
Leakage condition	Load torque (N·m)		
	Simulation value	Experiment value	Difference
5% Leakage	50	54.7	9.4%
10% Leakage	50	53.5	7.0%

From Table 3 and Table 4, we see that rotational speed of the hydraulic motor decreases and the load torque of the hydraulic motor increases in the experiment than in the simulation. The reasons of are following:

(a) Since detecting elements are installed in the hydraulic line, the hydraulic system damping will increase;

(b) Due to the impurity in hydraulic oil, friction damping in hydraulic components will increase;

(c) After the long-running of hydraulic motor, it will lead to wearing between the rotor and the stator of hydraulic motor.

Through the comprehensive analysis, it can be known that the experiment result agrees better with the simulation result under different leakage ratios of the hydraulic motor. The analysis results show that the leakage ratio of the hydraulic motor is sensitive to the rotational speed and load torque of the drilling rig, and the smaller the leakage ratio, the greater its influence on the rotational speed and load torque of the hydraulic motor.

CONCLUSIONS

Considering the influence of coupling relationships among electric control system, mechanical system and hydraulic system on the response of the hydraulic rig, a mechanical-electrical-hydraulic coupling dynamics model of the drilling rig was established by coupling method of the capacity conservation. Based on the model, the dynamic response of the drilling rig and leakage sensitivity of the hydraulic motor were analyzed by simulation, and the simulation results showed that the output characteristics of the model are in better agreement with the actual output response of the drilling rig. The rotational speed of the drilling rig will decrease obviously under larger load and hydraulic motor leakage amount. Then, drilling experiments were performed to verify the accuracy of the coupling dynamics model. Specially the sensitivity of the leakage ratio of the hydraulic motor to the output speed and load torque of the drilling rig were also studied experimentally. The research showed that the rotational speed and load torque of the drilling rig are very sensitive to the leakage ratio of the hydraulic motor.

ACKNOWLEDGMENT

Financial support for this work was provided by Sichuan Province Basic Research Plan Project under Grant No. 2013JY0165, the Key Research Project of Sichuan Province Department of Education, Cultivating Programme of Excellent Innovation Team of Chengdu University of Technology under Grant No. KYTD201301 and National Training Program of Innovation and Entrepreneurship for Undergraduates under Grant No. 201510616034.

REFERENCES

D. Wen, X. Shang, P. Gu, Z. Shi, W. Zheng, “Analysis of leakage and volumetric efficiency and seal improvement for double-stator swing hydraulic motor,” *Transactions of the Chinese Society of Agricultural Engineering*, Vol.33,No.12,pp.74-81(2017).

D.Z. Xin, X.S. Gong, Q.F. Wang, “Dynamic clamping theory of chuck used in collieries drilling rig based on load self-adaptation,” *Journal of China Coal Society*, Vol.38,No.3,pp.498-504(2013).

J.M. Zhang, Q.X. Liu, H.L. Tian, “Performance analysis of hydraulic control for kilometer directional rig used in underground coalmine,” *Journal of China Coal Society*, Vol.37, No.2,pp.341-345(2012).

Q.F. Wang, C.C. Zhu, C.B. Shi, “Dynamic characteristics of a drilling rig's driving head transmission system under varying working environment,” *Journal of Vibration and Shock*, Vol.33,No.17,pp.18-23(2014).

Q.F. Wang, C.C. Zhu, “Dynamic characteristics of a ZYWL-6000D full hydraulic directional drilling rig,” *Journal of Vibration and Shock*, Vol.33,No.15,pp.174-179(2014).

Q.Q. Wu, L.K. Zhang, Z.Y. Ma, “A model establishment and numerical simulation of dynamic coupled hydraulic–mechanical–electric–structural system for hydropower station,” *Nonlinear Dynamics*, Vol.87,No.1,pp.459-474(2017).

S.H. Ham, M.I. Roh, J.W. Hong. “Dynamic effect of a flexible riser in a fully connected semisubmersible drilling rig using the absolute nodal coordinate formulation.” *Journal of Offshore Mechanics and Arctic Engineering-Transctions of the ASME*, Vol.139,No.5,pp.051705(2017).

W.J. Yang, P. Norrlund, C.Y. Chung, J.D. Yang, U. Lundin, “Eigen-analysis of hydraulic-mechanical-electrical coupling mechanism for small signal stability of hydropower plant,” *Renewable Energy*, Vol.115,pp.1014-1025(2018).

X. Wang, M. Zhang, G. Man, “Fluid simulation of internal leakage for continuous rotary electro-hydraulic servo hydraulic motor,” *High Technology Letters*, Vol.22,No.4,pp.454-460(2016).

X.J. Wang, G.J. Man, M.J. Zhang, “Research on the leakage of continuous rotary electro-hydraulic servo hydraulic motor based on fluid structure interaction analysis,” *Industrial Lubrication & Tribology*, Vol.70,No.3,pp.544-551(2018).

Y.Z. Qi, L.G. Ouyang, Z.Y. Geng, S.T. Zhou, H.W. Huang, “Joint simulation and optimization of the lifting platform of anti-riot vehicles based on the mechanical-hydraulic system,” *International Conference on Smart Grid and Electrical Automation*, pp.497-500(2017).

Z.H. Meng, Q.L. Zeng, L. Wan, P. Liu, “Pose adjusting simulation of hydraulic support based on mechanical-electrical-hydraulic coordination," *Tehnicki Vjesnik-Technical Gazette*, Vol.25,No.4,pp.1110-1118(2018).

液壓鑽機機電液耦合動力學

陳光柱, 蔣成林, 苗長偉, 付林, 齊良釗
成都理工大學核技術與自動化工程學院

摘要

液壓鑽機作為一個機電液耦合的複雜機械系統,其耦合關係對其工作效能至關重要。液壓馬達做為鑽機的直接驅動部件, 內部容易出現洩漏，並且難以直接觀測，曰此, 分析液壓馬達內部洩漏條件下鑽機的工作效能尤為重要。本文對全液壓鑽機在空載和空載條件下的機−電−液的動力特性進行了分析。首先從理論上建立了鑽機的耦合動力學模型，然後通過模擬分析了鑽機的動態響應。其次，對液壓馬達進行洩漏敏感度模擬分析,探討液壓馬達內部洩漏對鑽機動態響應的影響。最後，搭建了鑽機動態響應測試平臺,在不同液壓馬達的洩漏率, 實驗結果與模擬結果吻合較好,液壓馬達的洩漏率對鑽機的轉速和負載轉矩非常敏感。